

signal per unit mass-2 ion current becomes, from (9),

$$S(2,D) = A(2,D)/I_2 \gtrsim [0.945Q(d,D) + 0.055Q(H_2^+,D)]. \quad (10)$$

Since the signal per unit ion current found when the proton beam crossed the deuterium atom beam is given by

$$S(1,D) = A(1,D)/I_1 \propto Q(p,D),$$

and the constant of proportionality is the same for the same neutral beam and geometry, we have

$$\frac{Q(d,D)}{Q(p,D)} = \frac{1}{0.945} \left[\frac{S(2,D)}{S(1,D)} - 0.055 \frac{Q(H_2^+,D)}{Q(p,D)} \right]. \quad (10a)$$

Similarly, when the neutral beam consists of D_2 rather than deuterium atoms, an identical argument yields the analogous formula

$$\frac{Q(d,D_2)}{Q(p,D_2)} = \frac{1}{0.945} \left[\frac{S(2,D_2)}{S(1,D_2)} - 0.055 \frac{Q(H_2^+,D_2)}{Q(p,D_2)} \right]. \quad (10b)$$

These two formulas were used in evaluating the cross-section ratios. The values for $Q(p,D)$, $Q(p,D_2)$, $Q(H_2^+,D)$, $Q(H_2^+,D_2)$ were taken as the values previously determined when the neutral beam consisted of light hydrogen atoms and molecules (as shown in Figs. 5, 3, 6, and 4, respectively) after it had been ascertained that the curves of relative cross section were the same

whether light or heavy hydrogen was used in the neutral beam.

The results of the measurements comparing proton and deuteron bombardment of the same neutral beam are shown in Figs. 7 and 8, where the data were handled according to Eqs. (10). When the deuterium molecule was the target (Fig. 7), the shift of the two curves along the energy axis could hardly have been in better agreement with the theoretical considerations presented above.

When the target system was the deuterium atom (Fig. 8), the expected shift was not observed. We cannot at the present time resolve the dilemma presented by the disagreement between the very convincing simple theoretical arguments and the equally convincing direct experimental data.

ACKNOWLEDGMENTS

We are indebted to a number of our colleagues, especially Dr. Samuel P. Cunningham and Dr. Donald W. Kerst, for their interest in these experiments and discussions of them. We are especially indebted to Professor D. R. Bates of Queen's University, Belfast, for his comments on the relation of these measurements to theory.

As always, the assistance of Miss Eugenia Rossell in the operation of the atomic beam apparatus has greatly accelerated the progress of these experiments.

Electron Spin Resonance of Atomic and Molecular Free Radicals Trapped at Liquid Helium Temperature*

C. K. JEN, S. N. FONER, E. L. COCHRAN, AND V. A. BOWERS
Applied Physics Laboratory, The Johns Hopkins University, Silver Spring, Maryland
 (Received June 17, 1958)

Electron spin resonance spectra of H, D, N, and CH_3 trapped in solid matrices at liquid helium temperature have been observed and interpreted. The effect of the matrix field on the resonance properties of the radicals has been investigated by depositing the radicals in matrices with different binding energies. The effect of the matrix on the g factor is extremely small in all cases. The deviation of the hyperfine coupling constant from the free-state value increases in a systematic way with increase in binding energy of the matrix, the percentage deviations being small for H, D, and CH_3 but rather large for the case of N. The widths and shapes of the spectral lines are discussed in terms of dipolar broadening, spin-lattice relaxation, anisotropic broadening, rate of passage and the modulation parameters used for observation.

Complex spectra, not adequately identified, have been observed from discharges in hydrogen and hydrogen-oxygen systems. Deductive evidence for an HO_2 resonance spectrum is presented.

The stable molecular free radicals O_2 , NO, and NO_2 have been studied. Only NO_2 yielded a positive result. Resonances for oxygen and chlorine atoms have been sought but not observed. It is suggested that radical species with orbital angular momenta may escape spin resonance observation because of matrix field anisotropy and that radical species with an even number of electrons may be unobservable because of crystalline field splitting resulting in a singlet ground level.

I. INTRODUCTION

FREE radicals trapped in solid media can be generated *in situ* by irradiation (uv, x-ray, γ -ray, electron, neutron, etc.) or can be generated in the

gaseous state and subsequently deposited in a suitable matrix. While the technique of stabilizing free radicals by isolating them in a rigid matrix is not new¹ and many frozen chemical systems have been examined

* This work supported by Bureau of Ordnance, Department of the Navy.

¹G. N. Lewis and D. Lipkin, *J. Am. Chem. Soc.* **64**, 2801 (1942).

for free radicals, the problem of detecting and identifying intermediates in a solid is complicated by matrix interactions, and only a few trapped free radicals have been identified with certainty. The spectra obtained with high-energy radiations, while quite interesting from a radiation damage standpoint, are not so readily interpretable as those obtained either by uv irradiation of the solid or by deposition from the gas state of systems whose radical content has been studied by other methods.

Electron spin-resonance techniques have been applied with great effectiveness to the study of trapped free radicals. The resonance method is inherently selective in detecting only those species with unpaired electron spins. Hyperfine structure in the resonance spectrum frequently permits an unambiguous identification of a free radical. However, there are many instances where the resonance spectra by themselves are inadequate to determine the identity of free radicals.

In this paper, electron spin resonance studies of a number of atomic and molecular free radicals trapped at liquid helium temperature are presented. The effect of the trapping matrix on the resonance spectra is examined. Also discussed are the instances where the resonance approach, as currently applied, has failed to give a positive result.

II. EXPERIMENTAL

A. Production of Free Radicals

Atomic and simple molecular free radicals are rather easily generated by electric discharges in appropriate gases. As the free radicals being studied increase in complexity, more selective methods of radical production, such as photolysis or photosensitization are needed to obtain specific radicals. While we have used all of

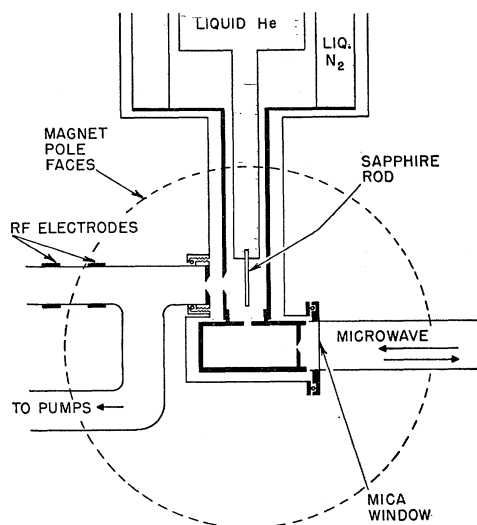


FIG. 1. Discharge system and low-temperature cell.

the above methods for free radical production, the principal method for the simple free radicals reported here was the electric discharge.

The free radicals were produced by an "electrodeless" discharge in a rapidly flowing gas stream. Two strips of aluminum foil wrapped around the quartz discharge tube (25-mm diameter) coupled the energy from an 8-Mc/sec transmitter into the gas. The power input to the discharge depended on the gases used and was set considerably higher for atom production, roughly 100 watts, than for production of molecular free radicals. The discharge products were pumped by a liquid nitrogen trapped mercury diffusion pump and fore-pump at a speed of about 1500 cm/sec past a short side tube connected to the low-temperature cell. The side tube was terminated by a glass slit which served as the source slit for a simple molecular beam system. The gas pressure in the discharge varied, depending on the particular experiment and on the size of the glass slit, but was usually about 0.1 mm Hg.

B. Low-Temperature Cell and Sample Deposition System

The general arrangement of the discharge system and the low-temperature cell is shown in Fig. 1. The upper portion of the low-temperature cell is essentially the metal Dewar system described by Duerig and Mador.² The sample is collected on a sapphire rod which is in direct thermal contact with liquid helium. The sapphire rod, 2 mm in diameter and 50 mm long, projects into the liquid helium reservoir through a vacuum-tight solder joint. Temperature of the sapphire rod is measured either by a 2.1% Co-Au, 0.37% Au-Ag thermocouple or by a 2.1% Co-Au, Chromel-*P* thermocouple soldered to a silver band on the sapphire about 2 mm below the vacuum joint. The liquid helium assembly can be raised or lowered mechanically by means of a siphon bellows arrangement.² Since liquid helium cooled surfaces are excellent pumps, there are four radiation baffled pumping slots (not shown) in the liquid nitrogen cooled radiation shield. Except for the slits used for sample deposition, the liquid helium assembly is surrounded by a liquid nitrogen radiation shield. The microwave cavity, shown in Fig. 1, is cooled to liquid nitrogen temperature by thermal contact with the radiation shield.

The sample deposition system is shown in detail in Fig. 2. The molecular beam from the glass slit is uncollimated and is condensed on the sapphire target. The discharge products can be condensed in various matrices by sending selected gases through the matrix slits at the same time the beam from the discharge is being deposited. The ratio of matrix to discharge products in the sample is typically of the order of 100:1. The glass slit varied in size from 0.5 mm \times 10 mm

² W. H. Duerig and I. L. Mador, *Rev. Sci. Instr.* **23**, 421 (1952).

(early experiments on hydrogen atoms³) to 0.11 mm \times 6 mm for most of the matrix effect experiments. The molecular beam flux to the sapphire target with the smaller slit is 3.8×10^{16} molecules/cm² sec for hydrogen molecules at 300°K and 0.10 mm Hg pressure. If the effective length of the sapphire target is taken as 1 cm and condensation is assumed perfect, then 1.4×10^{19} hydrogen molecules would be condensed in a 30-minute run. This would correspond to a layer about 2.6×10^{-3} cm thick. After the sample has been deposited, the sapphire rod is lowered into the microwave cavity.

C. Microwave Equipment

A rectangular microwave cavity of the reflecting type is used and resonates in the TE_{012} mode at a frequency of around 9178 Mc/sec. The cavity is electroformed and has internal dimensions of a 1-wavelength section of standard X -band wave guide. The sample-rod entrance

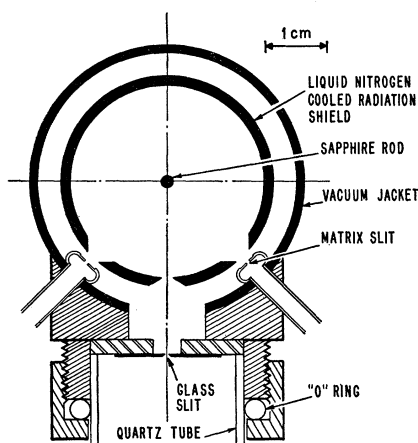


FIG. 2. Sample deposition system. Cross-section view of the slit system.

hole (5-mm diameter) is located at the center of the surface which allows the inserted sample to occupy the position of maximum microwave field intensity. The penetration of the sample rod into the cavity is adjustable up to a maximum of 16 mm. A microwave iris window (4.9-mm diameter) is located at the center of one end plate, the wall thickness being tapered to a thin edge at the aperture. The wave guide is extended a quarter wavelength beyond the iris and terminates to provide a vacuum gap between the liquid nitrogen cooled cavity and the room temperature coupling wave guide. A mica window is placed in the room temperature wave guide to maintain the cell vacuum. The unloaded Q of the cavity is about 18 000 at liquid nitrogen temperature and the window Q , controlled by the iris aperture, is chosen to make the ratio of the unloaded Q

³ Jen, Foner, Cochran, and Bowers, *Phys. Rev.* **104**, 846 (1956).

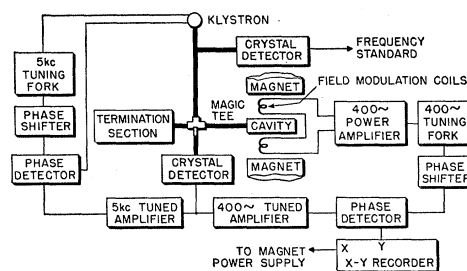


FIG. 3. Block diagram of the microwave system.

to the window Q about 0.4, which is close to the condition for maximum sensitivity for detection.

The microwave system used is shown in Fig. 3. In many respects the system is conventional for an electron spin resonance spectrometer. The klystron is stabilized at the sample cavity resonance frequency by a servo-loop using the discriminator characteristic of the cavity relative to a small-frequency modulation of the klystron. The microwave frequency is measured with a Hewlett-Packard electronic counter and transfer oscillator system which is standardized with radio station WWV.

D. Magnetic Field and Signal Recording

A 12-inch Varian magnet with 3-inch gap supplies the magnetic field. The microwave cavity is placed in the central and most homogeneous region of the magnet. The magnetic field is measured with a proton resonance magnetometer with the probe placed as close as possible to the center of the cavity (3 cm). The difference between the fields at the sample and the magnetometer probe is a very small known quantity, negligible for most of our measurements.

A magnetic field modulation of 400 cps is used. The modulation is supplied by a pair of pancake coils outside the vacuum jacket surrounding the cavity. With this arrangement the field has to penetrate both the brass vacuum wall and the copper cavity. With reasonable power, modulation fields of several oersteds amplitude can be obtained. The resonance of a sample appears at the output of the crystal detector as a signal at the modulation frequency. This signal is amplified, phase detected, and fed into an X - Y recorder. For resonance observations, the magnetic field is slowly swept over the desired range in two to ten minutes. The direction of sweep is alternately reversed in taking data.

The sensitivity of the apparatus with the sample at liquid helium temperature was measured by using a known amount of DPPH (diphenyl picryl hydrazyl) on the end of the sapphire rod. It is conservatively estimated that the sensitivity is 10^{-11} mole of DPPH or about 6×10^{12} spins for a line having a half-width of about 4 oersteds.

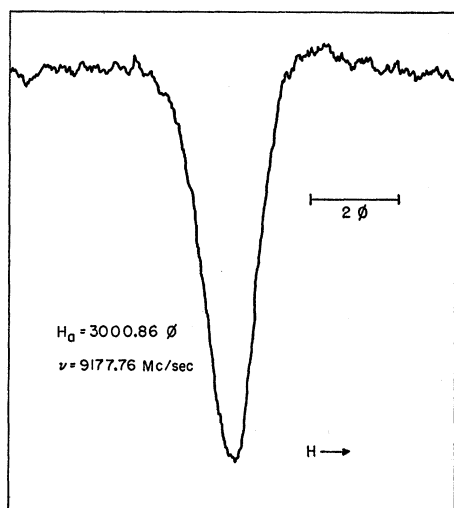


FIG. 4. Low-field line of the doublet spectrum for H in H_2 matrix. Detector phase at 90° with respect to the field modulation. In this and other figures, the symbol ϕ is used to denote oersteds.

III. RESONANCE SPECTRA OF TRAPPED ATOMIC FREE RADICALS

A. Observed Spectra of Hydrogen, Deuterium, and Nitrogen Atoms

Results obtained from the observation of the electron spin resonance of trapped hydrogen, deuterium, and nitrogen atoms have been briefly reported before.^{3,4} A somewhat more detailed description of these cases will be given here. In addition, an unsuccessful search for the resonances of oxygen and chlorine atoms will be mentioned. The effect of different matrices on the resonance characteristics will be deferred to Sec. V, where atomic and molecular free radicals are jointly considered.

Hydrogen Atoms

The observed hyperfine spectrum for hydrogen atoms trapped in a solid matrix is a doublet which is very nearly the same as that observed for free hydrogen atoms in the gaseous state. Figure 4 shows a trace of the low-field line, which has the same spectral shape as the high-field line, for hydrogen atoms in an H_2 matrix. The field positions of the two lines at a fixed microwave frequency are given in Table I.

The spectral shape of the line in Fig. 4 is not a slow passage presentation of an absorption line detected with field modulation.⁵ The result may be interpreted

⁴ Foner, Jen, Cochran, and Bowers, *J. Chem. Phys.* **28**, 351 (1958).

⁵ The spectral shape of an absorption line detected with field modulation under slow passage conditions is usually in the form of the derivative of the absorption coefficient. The absorption signal at the modulation frequency is in phase with the modulation field. If, however, there is a long spin-lattice relaxation time (T_1) and a high modulation angular frequency (ω_m) such that $\omega_m T_1 \gg 1$, the absorption signal has also a component in phase quadrature

as a fast passage phenomenon brought about by a long spin-lattice relaxation time of the sample and a relatively high modulation frequency. Additional evidence for a long spin-relaxation time is the observation that the hydrogen lines show the effect of intensity saturation even with the smallest microwave magnetic field used (5×10^{-3} oersted).

Deuterium Atoms

Consistent with the doublet spectrum for hydrogen atoms, the observed hyperfine spectrum for trapped deuterium atoms is a triplet. Figure 5 shows a trace for the center line, which is also generally representative in appearance of the higher and lower field lines. The field positions of the three lines at a fixed microwave frequency are given in Table I.

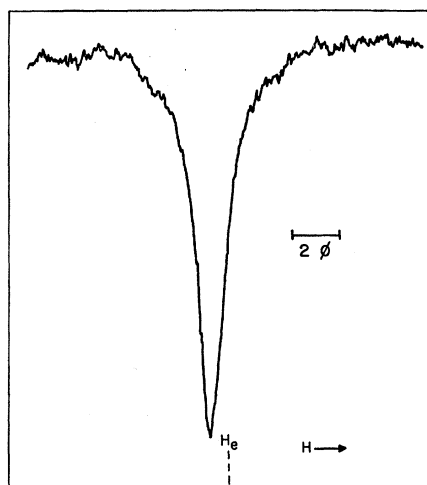


FIG. 5. Center line of the triplet spectrum for D in D_2 matrix. Detector phase at 90° with respect to the field modulation. In this and following figures, H_e stands for the free electron resonance field given by the relation $h\nu = g_e \mu_0 H_e$ with $g_e = 2.00230$.

The spectral shape of a deuterium line is similar to that of a hydrogen line though somewhat broader. This spectral presentation, together with the easy saturability of a deuterium line, again suggests the presence of a fairly long spin-lattice relaxation time. There is, in addition, an apparent anomaly in the intensity distribution among the triplet components. The ratio of the peak intensity of the center component to that of either side component varies from about 4 at a high microwave power level to about 1.5 at the lowest detectable power. This ratio should be unity according to the theory for free atoms. We shall comment on an explanation of this anomaly in a later section.

with the modulation field, particularly if the line is partially saturated [see A. M. Portis, *Phys. Rev.* **100**, 1219 (1955); A. G. Redfield, *Phys. Rev.* **98**, 1787 (1955)]. It seems that under certain conditions, a field-modulated absorption curve at fast passage can look like a field-modulated dispersion curve at slow passage.

Nitrogen Atoms

In agreement with the known spectrum of a free nitrogen atom, the observed hyperfine spectrum for this atom in the trapped state is a closely spaced triplet as shown in Fig. 6.† The field positions for nitrogen atoms in an N₂ matrix are tabulated in Table I.

In contrast to the cases of hydrogen and deuterium atoms, the spectrum in Fig. 6 shows a normal differentiated absorption line shape typical of a slow passage condition. There is also an even intensity distribution among the triplet components in accordance with theory.

B. Theory of the Hyperfine Spectra of Free Atoms in S States

The magnetic resonance properties of atoms are well known both theoretically and experimentally. We shall state the essential theoretical results for an S-state atom, which is the simplest as well as the only relevant case for the present considerations. Let **J** be the total electronic angular momentum and **I** be the angular momentum of the nucleus. Then the spin Hamiltonian

TABLE I. Resonant magnetic fields (oersteds) of H, D, and N trapped in H₂, D₂, and N₂ matrices, respectively. ν =microwave frequency (Mc/sec).

Atom	H _a	H ₀	H _b	ν
H	3000.86		3509.55	9177.76
D	3196.42	3273.13	3351.83	9178.47
N	3270.96	3275.26	3279.58	9177.68

\mathcal{H} for an atom in a magnetic field **H** is

$$\mathcal{H} = g_J \mu_0 \mathbf{J} \cdot \mathbf{H} + g_I \mu_0 \mathbf{I} \cdot \mathbf{H} + A \mathbf{J} \cdot \mathbf{I}, \quad (1)$$

where g_J =electronic g factor (absolute value), g_I =nuclear g factor, defined by $g_I = -\mu_I / (\mu_0 I)$, μ_0 =Bohr magneton, and A =hyperfine coupling constant.

For an atom in a $^2S_{1/2}$ state (such as an H or D atom), the solution of Eq. (1) for the magnetic energy levels is given by the Breit-Rabi formula,^{6,7}

$$W_{I \pm \frac{1}{2}} = -\frac{\Delta W}{2(2I+1)} + g_I \mu_0 H M \pm \frac{\Delta W}{2} \left(1 + \frac{4Mx}{2I+1} + x^2 \right)^{\frac{1}{2}}, \quad (2)$$

where $\Delta W = \frac{1}{2}(2I+1)A$ which is the hyperfine energy

† Note added in proof.—Under certain experimental conditions we have observed for N in N₂ four weak satellite lines, two on each side of the main triplet, similar to those reported by T. Cole and H. M. McConnell, *J. Chem. Phys.* **29**, 451 (1958). The satellites were not observed in our slow deposition experiments. However, they were seen when the sample deposition rate was high suggesting that the occurrence of satellites is related to the crystalline order of the N₂ matrix.

⁶ G. Breit and I. I. Rabi, *Phys. Rev.* **38**, 2082 (1931).

⁷ J. E. Nafe and E. B. Nelson, *Phys. Rev.* **73**, 718 (1948).

separation, M =magnetic quantum number of $\mathbf{F} = \mathbf{J} + \mathbf{I}$, and $x = (g_J - g_I)\mu_0 H / \Delta W$. In this case, the quantity A is, by the Fermi formula,^{8,9}

$$A = \frac{16\pi}{3} \frac{\mu_I}{I} |\psi(0)|^2 = -\frac{16\pi}{3} g_I \mu_0^2 |\psi(0)|^2, \quad (3)$$

where $\psi(0)$ =wave function of an S electron at the nucleus.

For an atom in a $^4S_{3/2}$ state (such as a nitrogen atom), solution for Eq. (1) can be carried out in a way similar to the derivation of Eq. (2), except that a cubic equation is involved in addition to a quadratic for $I=1$. However, for $A \ll \mu_0 H$, the solution can be most easily obtained by the perturbation method with the result

$$W(M_J, M_I) = M_J g_J \mu_0 H + M_I g_I \mu_0 H + A M_J M_I + A^2 f(M_J, M_I), \quad (4)$$

where

$$f(M_J, M_I) = \frac{1}{2(g_J - g_I)\mu_0 H} [M_J \{I(I+1) - M_I^2\} - M_I \{J(J+1) - M_J^2\}]. \quad (5)$$

For a nitrogen atom, with the configuration $1s^2 2s^2 (2p)^3 ^4S_{3/2}$, the hyperfine coupling constant A would be zero if the electrons with unpaired spins were all in pure $2p$ orbitals. However, when one allows for configuration interaction, with the resulting admixture of a $3s$ orbital, then the coupling constant will assume an appropriate nonzero value.

The general selection rules for the transition between two states are: $\Delta F = \pm 1$ or 0 and $\Delta M = \pm 1$ or 0. However, for most magnetic resonance experiments, the

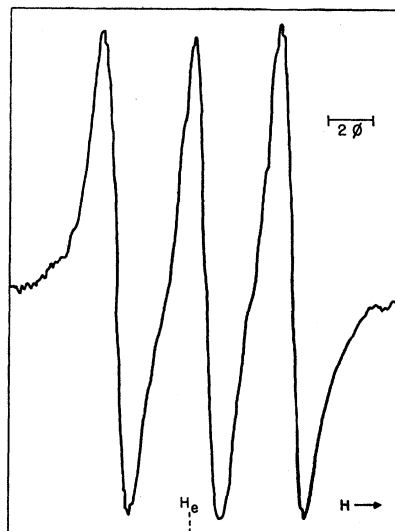


FIG. 6. Triplet spectrum of N in H₂ matrix.

⁸ E. Fermi, *Z. Physik* **60**, 320 (1930).

⁹ E. Fermi and E. Segrè, *Z. Physik* **82**, 729 (1933).

steady magnetic field is high enough so that a large measure of the Paschen-Back condition is attained. Under these conditions, the allowed transitions are governed by the selection rules: $\Delta M_J = \pm 1$ and $\Delta M_I = 0$. Any forbidden transition should be very much less intense than the allowed ones.

C. Interpretation of the Hyperfine Spectra of Trapped Atoms

One basic approach to the problem of interpreting the hyperfine spectrum of a trapped atom is to solve the problem in which the total Hamiltonian contains the terms in Eq. (1) for the free atom plus another term which describes the interaction energy between the atom and the solid matrix. Such a solution is at present not feasible, because we do not have a detailed knowledge of the fields in the neighborhood of the trapped atom, not to speak of the computational difficulties that may be involved. Another approach is to apply the known solutions for a free atom, such as in Eq. (2) or Eq. (4), to the case of a trapped atom with the quantities g_J and A treated as effective values in a given medium. Thus, the effect of a matrix field can be regarded as being embodied in the measured departures of g_J and A in the trapped state from those in the free state. This procedure will be adopted for all the interpretations in this paper.

H in H₂ Matrix

There are two allowed transitions (with each participating state designated by its F, M value): $(0, 0 \rightarrow 1, 1)$ and $(1, -1 \rightarrow 1, 0)$ which should correspond to the observed low-field and high-field lines at a constant microwave frequency. Application of Eq. (2) to these transitions gives two equations, from which the values for g_J and ΔW can be uniquely determined with $I(\text{H}) = \frac{1}{2}$, $g_I(\text{H}) = -3.04 \times 10^{-3}$ and the data in Table I for the microwave frequency and the two resonance fields. The results of such a calculation are shown in Table II together with the corresponding known values for the free hydrogen atom. From the evidence presented we have secured an unambiguous identification of trapped

TABLE II. g factors, hyperfine energy separations (ΔW) and/or hyperfine coupling constant (A) of H, D, and N trapped in H₂, D₂, and N₂ matrices, respectively.^a

Atom	Matrix	g_J	ΔW (Mc/sec)	A (Mc/sec)
H	free ^{b,c}	2.002256(24)	1420.40573(5)	1420.40573(5)
H ₂		2.00230(8)	1417.11(20)	1417.11(20)
D	free ^d	2.002256(24)	327.384302(30)	218.256201(20)
D ₂		2.00231(8)	326.57(27)	217.71(18)
N	free ^e	2.00215(3)		10.45(2)
N ₂		2.00200(8)		12.08(12)

^a The numbers in parentheses indicate experimental and/or conversion errors in the last figures of the associated values.

^b P. Kusch, Phys. Rev. **100**, 1188 (1955).

^c R. Beringer and M. A. Heald, Phys. Rev. **95**, 1474 (1954).

^d A. G. Prodel and P. Kusch, Phys. Rev. **79**, 1009 (1950); **88**, 184 (1952).

^e M. A. Heald and R. Beringer, Phys. Rev. **96**, 645 (1954).

hydrogen atoms as the origin of the observed doublet spectrum. Furthermore, on the basis of their magnetic properties, the trapped atoms can be considered to be very nearly, but not completely, free.

D in D₂ Matrix

There are three allowed transitions (with each state designated by its F, M value): $(\frac{1}{2}, \frac{1}{2} \rightarrow \frac{3}{2}, \frac{3}{2})$, $(\frac{1}{2}, -\frac{1}{2} \rightarrow \frac{3}{2}, \frac{1}{2})$ and $(\frac{3}{2}, -\frac{3}{2} \rightarrow \frac{3}{2}, -\frac{1}{2})$. These transitions with the aid of Eq. (2) give three equations for the determination of only two unknowns: g_J and ΔW . We also use the known quantities: $I(\text{D}) = 1$, $g_I(\text{D}) = -4.67 \times 10^{-4}$, and the data in Table I for the deuterium atom. The results of calculation, affirmed by over-determination, are shown in Table II, together with the known values for the free deuterium atom. It is seen that the

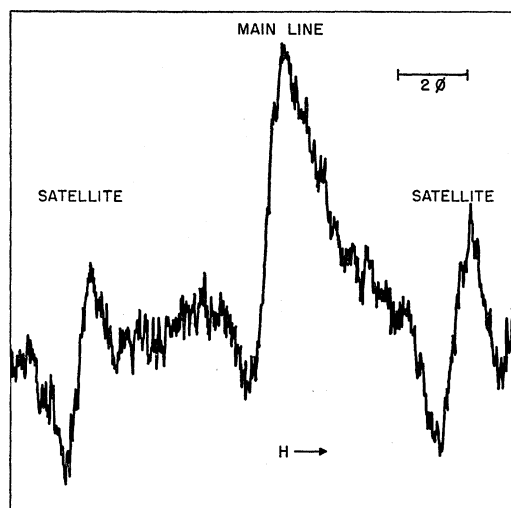


FIG. 7. Satellite lines accompanying the H high-field line.

constant g_J is, similar to the case of the hydrogen atom, hardly affected by the solid matrix and that the hyperfine energy for a trapped deuterium atom is slightly reduced by a D₂ matrix in much the same proportion as that for a trapped hydrogen atom by an H₂ matrix. This result seems reasonable from the point of view that D₂ and H₂ solids have quite comparable binding energies.

Furthermore, it is worth noting that the Fermi formula [Eq. (3)] predicts, aside from a possible small hyperfine anomaly, $A_{\text{H}}(\text{free})/A_{\text{D}}(\text{free}) = g_I(\text{H})/g_I(\text{D})$ and experimentally we find $A_{\text{H}}(\text{trapped})/A_{\text{D}}(\text{trapped}) = g_I(\text{H})/g_I(\text{D})$ to within 0.017%. If we regard the Fermi formula as being applicable to trapped atoms, then the experimental result implies that the quantity $|\psi(0)|^2$ for a trapped hydrogen atom is very nearly the same as for a trapped D atom. If, on the other hand, we conclude from the physics of the situation that $|\psi(0)|^2$ should be very nearly the same for trapped hydrogen and deuterium atoms, then the experimental

result implies that the Fermi formula gives a correct description of the hyperfine interaction of trapped atoms in the S state.

N in N_2 Matrix

The hyperfine coupling energy for a nitrogen atom in the $^4S_{3/2}$ state is small enough so that Eq. (4) is quite adequate for the description. Using, for convenience, the high-field designation (M_J, M_I) for a magnetic level, there are twelve energy levels, with M_J assuming any of the values: $-\frac{3}{2}, -\frac{1}{2}, \frac{1}{2}, \frac{3}{2}$, and M_I assuming any of the values: $-1, 0, 1$, since $I(N^{14})=1$. There are nine transitions of the type $(M_J, M_I \rightarrow M_J \pm 1, M_I)$; but they actually fall into three groups, each designated by a constant M_I . The separation among the three lines in each group, which is determined by the A^2 term in Eq. (4), is extremely small and is not resolved in the present measurements. The constants g_J and A are given by

$$g_J = \frac{\nu}{(\mu_0/h)H_0} \left[1 - \left(\frac{\Delta H}{H_0} \right)^2 \right], \quad (6)$$

$$A = \frac{\Delta H}{H_0} \nu, \quad (7)$$

where ν =microwave frequency, H_0 =magnetic field of the center line, ΔH =average separation of adjacent lines and h =Planck's constant. Since $(\Delta H/H_0)^2=1.7 \times 10^{-6}$, the expression for g_J [Eq. (6)] can be replaced by the simpler expression

$$g_J = \frac{\nu}{(\mu_0/h)H_0}. \quad (8)$$

The results for trapped nitrogen atoms are shown in Table II together with the known values for the free nitrogen atom. It is seen that g_J is very slightly affected by the matrix but that the hyperfine coupling constant is larger for a trapped nitrogen atom than for a free atom, in contrast to the cases of hydrogen and deuterium where the coupling constant is smaller for the trapped atom.

D. Satellite Lines in the Hyperfine Spectra of Trapped Atoms

Satellite lines were observed in the hyperfine spectra of hydrogen and deuterium atoms trapped in their parent molecular matrices. They were usually very much weaker in intensity than the main lines and were observed only when the microwave power level was high enough to heavily saturate the main lines.

In the case of hydrogen atoms in a molecular hydrogen matrix, each of the two hydrogen lines was accompanied by two satellite lines symmetrically placed relative to the main line. A trace of such a spectrum is shown in Fig. 7. The separation in magnetic field between either satellite and the main line is equal, within

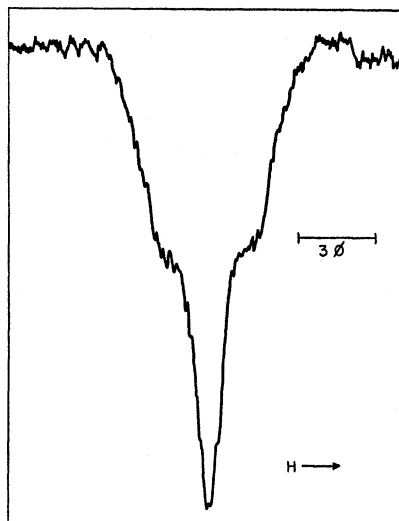


Fig. 8. Unresolved satellite structure of the D high-field line.

measurement error, to $(g_I/g_J)H_0$, where H_0 is the resonance field of the main line.

In the case of deuterium atoms in molecular deuterium, each of the three deuterium lines shows an unresolved structure which indicates the presence of satellites, as illustrated in Fig. 8. The satellite separation in D should be smaller than in H by the factor $g_I(H)/g_I(D)=6.5$. Because of the unresolved picture, the field positions of the satellites cannot be determined accurately. A rough estimate indicates that there are two pairs of satellites centered around each main line. The field separation between the main line and either line in the first pair is approximately $(g_I/g_J)H_0$ and the corresponding value in the second pair is approximately $2(g_I/g_J)H_0$.

Satellite lines in the resonance spectrum of hydrogen atoms have been observed before by Zeldes and Livingston¹⁰ under somewhat different conditions. Their presence was interpreted as evidence for a mechanism in which the spin of a neighboring proton is flipped simultaneously with the electron of the hydrogen atom. A similar explanation would seem reasonable for our observations. In the present case, the atomic electron may be assumed to be coupled to the protons in a neighboring hydrogen molecule. A flip of electron spin could cause a simultaneous change in orientation of the two parallel nuclear spins of ortho-hydrogen with the change of Zeeman energy as observed. The flip of a single proton spin simultaneously with the electron spin flip is considered unlikely since this would involve the conversion of para- to ortho-hydrogen or vice versa, a process which involves a large energy change because of the large energy separation (121 cm^{-1}) of the $J=0$ and $J=1$ rotational ground states of these two species. A similar picture would hold for deuterium atoms in a

¹⁰ H. Zeldes and R. Livingston, Phys. Rev. **96**, 1702 (1954).

deuterium matrix with the additional possibility of induced transitions with $\Delta M_I = \pm 2$, corresponding to a field separation of $2(g_I/g_J)H_0$, as a result of deuteron quadrupole coupling. Because of the unresolved spectrum for deuterium satellites, there is some uncertainty in the experimental evidence for this additional effect.

E. Attempts to Observe Resonance Spectra of Trapped Oxygen and Chlorine Atoms

Oxygen¹¹ and chlorine¹² are *P*-state atoms whose magnetic properties in the free state are well known but which have not been observed in the trapped state. In this work, several experiments have been performed for each atom by depositing the discharge products of the parent gas in several matrices such as H₂, A, or Cl₂ (for chlorine discharge). A wide range of the magnetic spectrum was searched, but no resonance lines were found in either case.

If the matrix effects were extremely small, the spectral patterns of oxygen and chlorine atoms would be similar to those of the free state atoms. An oxygen atom in the ³P₂ ground state and nuclear spin $I(\text{O}^{16})=0$ is expected to give a single line with four unresolved components at the field corresponding to $g_J = \frac{3}{2}$. A chlorine atom in the ²P_{3/2} ground state and nuclear spin $I(\text{Cl}^{35})=I(\text{Cl}^{37})=\frac{3}{2}$ is expected to give a hyperfine magnetic spectrum consisting of twelve lines for each isotope, in four equally spaced groups of three closely spaced lines, centered around the field corresponding to $g_J = 4/3$.

The absence of resonance spectra is evidence that the matrix field is very potent in its effect on *P*-state

atoms. The matrix field may partially quench the electronic orbital angular momentum. It also may split some degenerate levels and leave only a singlet ground level for an atom with an even number of electrons. The possibility of splitting to give a singlet nonmagnetic ground level may explain the failure to observe resonances for the oxygen atom. On the other hand, there should still be a Kramers' degeneracy for the ground level of the chlorine atom because it has an odd number of electrons. To explain the failure to observe resonance in this case, it is reasonable to assume that the interaction between the matrix field and the orbital angular momentum produces a large enough magnetic anisotropy to broaden the resonance lines beyond recognition.

IV. RESONANCE SPECTRA OF TRAPPED MOLECULAR FREE RADICALS

Molecular free radicals can be divided into two classes: (a) unstable molecules, and (b) stable paramagnetic molecules, exemplified by a very small number of species like O₂, NO, NO₂, etc. Magnetic resonance studies have been made of the stable molecules mentioned above in the gaseous state, but, as yet, very little study has been made of unstable molecules.

A large number of magnetic resonance spectra of free radicals trapped in solids have been reported. The identification of the species responsible for the spectra is, however, not a simple matter and in many cases may not be definitive. In this section a comprehensive study of the methyl radical is presented. Complex spectra whose identities are uncertain are then considered. Also for purposes of comparison and evaluation, results for a few stable molecular radicals under trapped conditions are discussed.

A. Methyl Radical

When the products of a very-low-power discharge in methane were condensed at 4.2°K, a four-line spectrum as shown in Fig. 9 was obtained. The same spectrum was also observed when a frozen sample of 1% CH₃I in argon was irradiated by 2537 Å mercury light. The field positions of the spectral lines at fixed microwave frequency are listed in Table III. The average separation between adjacent lines is 22.9 oersteds. The intensity distribution among the spectral lines in Fig. 9 is approximately 1:2.2:2.2:1. As the sample was slowly warmed from 4.2°K, the intensity of the lines increased, they became narrower, and the intensity distribution approached the ratio 1:3:3:1. Above about 8°K, the entire spectrum weakened with increasing temperature as expected from the temperature effect on susceptibility. However, the positions of the lines remained unchanged during warmup. We deduce from this that the spectrum at 4.2°K shown in Fig. 9 is probably power saturated and if we were able to obtain an unsaturated spectrum at 4.2°K, the line ratio would be 1:3:3:1.

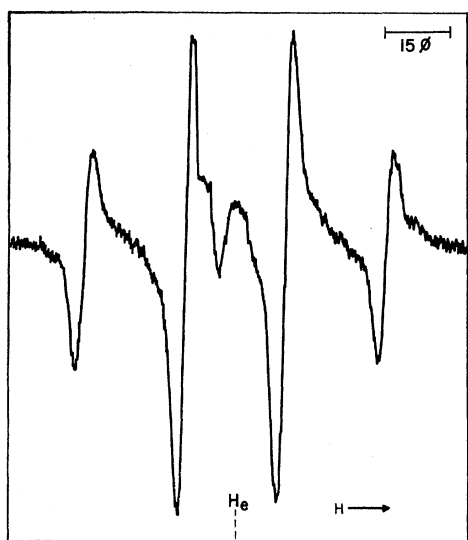


FIG. 9. Quartet spectrum of CH₃ in CH₄ matrix at 4.2°K. Small line near the center of the spectrum is due to a calibration sample of DPPH.

¹¹ E. B. Rawson and R. Beringer, Phys. Rev. **88**, 677 (1952).

¹² Davis, Feld, Zabel, and Zacharias, Phys. Rev. **76**, 1076 (1949).

TABLE III. Resonant magnetic fields, g_J and A for CH_3 in CH_4 matrix.^a $\nu=9177.85$ Mc/sec.

Resonant fields (oersteds)				g_J	A (Mc/sec)
3240.11	3262.89	3285.96	3308.95	2.00242(8)	64.39(18)

^a The numbers in parentheses indicate experimental and/or conversion errors in the last figures of the associated values.

The observed spectrum is consistent with the interpretation that it is produced by CH_3 radicals trapped in a solid matrix. The quartet is expected from the hyperfine interaction of an unpaired electron with three protons, each having a nuclear spin of $\frac{1}{2}$. The observed intensity distribution under unsaturated conditions is in agreement with the 1:3:3:1 statistical distribution of nuclear spins.

In another experiment, a spectrum was obtained from the discharge products of partially deuterated methane. The spectrum was quite complicated. It was possible, however, to assign all the observed lines to the isotopic forms of the methyl radical (CD_3 , CD_2H , CHD_2 , and CH_3) by supposing the hyperfine contribution of a deuteron is reduced from that of a proton by the factor $g_I(\text{D})/g_I(\text{H})$.

An elementary analysis of the CH_3 problem can be made in a way analogous to previous considerations for an atom. We have for the spin Hamiltonian

$$\mathcal{H} = g_J \mu_0 \mathbf{J} \cdot \mathbf{H} + g_I \mu_0 \sum_i \mathbf{I}_i \cdot \mathbf{H} + \sum_i A_i \mathbf{J} \cdot \mathbf{I}_i, \quad (9)$$

where \mathbf{J} is, as before, the angular momentum of the unpaired electron and i denotes the i th hydrogen nucleus. If all three hydrogen nuclei are equivalent, we can write the last term in Eq. (9) as

$$\mathcal{H}_{\text{hf}} = A \mathbf{J} \cdot \sum_i \mathbf{I}_i. \quad (10)$$

If $\mu_0 H \gg A$, then the expectation value of the energy for Eq. (9) is to the second-order approximation:

$$W = M_J g_J \mu_0 H + M_I g_I \mu_0 H + A M_I M_J + A^2 F(M_J, M_I), \quad (11)$$

where $M_I = \sum_i m_i$, $m_i = \pm \frac{1}{2}$, $M_J = \pm \frac{1}{2}$, and¹³

$$F(M_J, M_I) = (3M_J - M_I) \frac{1}{4(g_J - g_I)\mu_0 H}. \quad (12)$$

We note that Eq. (11) for a molecular free radical having equivalent magnetic nuclei is formally the same as Eq. (4) for an atom, provided the second-order correction (the A^2 term) is negligible. However, the intensity distribution of the spectral lines for a molecule is quite different from that of an atom because of the difference in the statistical weights for a given M_I .

By applying Eqs. (11) and (12) and the selection rules $\Delta M_J = \pm 1$ and $\Delta M_I = 0$, values for g_J and A pertaining to CH_3 in a CH_4 matrix have been calculated, with the results shown in Table III.

¹³ Equation (12) is not a general equation for all values of M_J and M_I but is restricted to the present special case.

While there is as yet no general theory for hyperfine interactions which directly applies to the CH_3 radical, McConnell¹⁴ has worked out a theory for isotropic hyperfine interactions in π -electron radicals which bears on this case. The relationship obtained by McConnell for the hyperfine coupling constant A , is

$$A = Q \rho_c, \quad (13)$$

where ρ_c is defined as the "unpaired electron density" at the carbon atom and Q is a semiempirical constant, $Q = -22.5$ oersted, assumed to be the same for all aromatic CH bonds. If we try this formulation for a methyl radical, taking ρ_c equal to unity, since there is only a single carbon atom, we obtain 22.5 oersteds for the numerical value of A . This is in good agreement with our measured value of 22.9 oersteds for CH_3 in a CH_4 matrix and indicates that the theory is applicable to this case.

B. Unidentified Spectrum from Hydrogen Discharge

Since the region around the free electron resonance field is not occupied by the atomic hydrogen lines, any new spectral system falling in this region can be studied without complication. In our first experiments with commercially pure hydrogen, a triplet spectrum was observed which was soon identified with nitrogen atoms formed in the discharge from the nitrogen impurity. These nitrogen lines disappeared when the hydrogen was purified either by diffusion through a heated palladium tube or by fractional distillation from a liquid helium cooled trap. With the highly purified hydrogen under certain conditions we obtained the four line spectrum shown in Fig. 10. The separation between

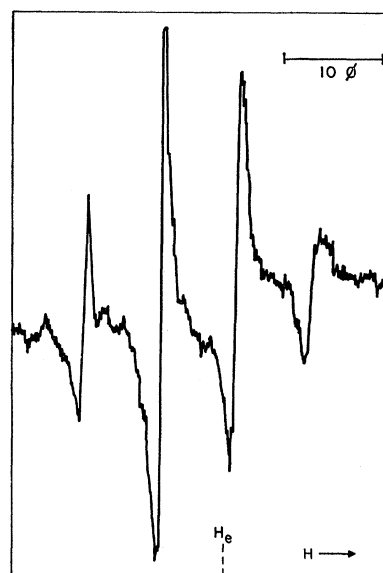


FIG. 10. An unidentified spectrum observed from the condensed products of a discharge in H_2 .

¹⁴ H. M. McConnell and D. B. Chesnut, J. Chem. Phys. 28, 107 (1958).

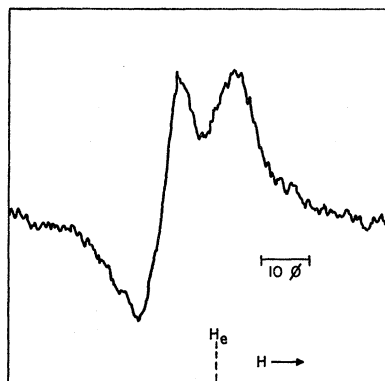


FIG. 11. A spectrum observed by condensing H_2O_2 discharge products in H_2 matrix. The spectrum is probably due to HO_2 .

adjacent lines is 7.3 oersteds, but the intensity distribution is quite asymmetrical. We do not have sufficient evidence to state that the spectrum in Fig. 10 is necessarily due to a single radical.

Because of the apparent quartet structure presented in Fig. 10, it has been speculated that the spectrum might be evidence for H_3 in the trapped state. Yet, the speculated presence of H_3 implies a similar situation for D_3 which, by the same reasoning, should give a seven-line spectrum with the line separation reduced by a factor of 6.5. A spectrum of this type was not found in a sample condensed from the deuterium discharge. The possibility that the spectrum was due to an impurity generated by the discharge cannot be completely excluded. Since hydrogen atoms can react with quartz to produce silane, SiH_4 , it was thought that the spectrum might, perhaps, be due to SiH_3 . This explanation was rendered unlikely, however, by the failure to observe the spectrum when silane was subjected to discharge.

C. Complex Spectrum in the Hydrogen-Oxygen System

Discharges in hydrogen-oxygen systems are potential sources of the free radicals H, O, OH, and HO_2 . The spectrum for hydrogen atoms has been discussed in detail. Negative results for trapped oxygen atoms have been described and negative results for trapped oxygen molecules will be described in the section on stable molecules. From these considerations, one concludes that any new spectrum is probably due to OH or HO_2 radicals.

A low-power discharge in H_2O_2 has been used by Foner and Hudson¹⁵ as a source of HO_2 radicals for mass spectrometric studies. They find that OH radicals are removed very rapidly by reaction with H_2O_2 , and within milliseconds after leaving the discharge the predominant free radical in the gas is HO_2 . Under conditions favorable for HO_2 production, the discharge products from H_2O_2 were condensed in an H_2 matrix.

¹⁵ S. N. Foner and R. L. Hudson, Symposium on Free Radicals, Laval University, Quebec, September 10, 1956 (unpublished). Also J. Chem. Phys. **23**, 1364 (1955).

The spectrum is shown in Fig. 11. It is essentially a broad asymmetrical line. The high-field lobe is seen to have a double-humped structure. A similar spectrum was also obtained from a discharge in H_2O .

There is no clear-cut explanation for this spectrum. From the resonance information alone we are unable to determine the origin of the spectrum. However, the spectrum is obtained in a system which is favorable for HO_2 production. Furthermore, the alternative possibility that the spectrum is due to OH is weakened by the negative results on trapped NO (discussed later) which has a similar electronic structure. The evidence, therefore, favors identification of the spectrum with HO_2 .

Similar resonances have been observed^{16,17} for the products of discharges in H_2O and related substances condensed at liquid nitrogen temperature. HO_2 was suggested as the radical responsible for the resonance line. This interpretation is supported by our observations.

D. Magnetic Spectra of Stable Free Radicals

The stable molecular free radicals NO_2 , NO, and O_2 were individually deposited in argon matrices at 4.2°K and examined for spin resonance.

NO_2

Since NO_2 has a ground state analogous to that of a $^2\Sigma$ molecule with an almost free electron spin, its resonance spectrum is expected to be a triplet for $I(N^{14})=1$. Castle and Beringer¹⁸ observed a spectrum of three broad peaks for NO_2 at a gas pressure of 5 to 15 mm Hg. The locations of the peaks could only be roughly determined and had an average separation of about 48 oersteds. At a lower pressure, each peak was partially resolved into a large number of lines, which were qualitatively interpreted as the rotational fine structure.

In this work, the resonant spectrum of NO_2 trapped in an argon matrix was observed with the result as shown in Fig. 12. The spectrum contains a recognizable triplet whose components are labelled as *a*, *b*, and *c* in the figure. But it also contains *d*, *e*, and *f* which have very little uniformity among themselves except approximately equal spacing. In another high resolution trace (not shown), *c* and *f* were seen to be separate lines but that *c* was broadened by a part of *f* which had a differentiated absorption curve.

The triplet formed by the lines *a*, *b* and *c* agrees with our expectations for the resonance spectrum of NO_2 in the trapped state. The center line position corresponds to a *g* factor of 2.0037. The average separation between adjacent lines is 57.8 oersteds corresponding to a hyperfine coupling constant (*A*) of 162 Mc/sec, which is 12% higher than the value reported by Castle and Beringer

¹⁶ Livingston, Ghormley, and Zeldes, J. Chem. Phys. **24**, 483 (1956).

¹⁷ Gorbonev, Kaitmazov, Prokhorov, and Tsentsiper, Zhur. Fiz. Khim **31**, 515 (1957).

¹⁸ J. G. Castle and R. Beringer, Phys. Rev. **80**, 114 (1950).

for free NO_2 . The difference between the two results may be partly due to the complicating effect of the rotational structure present in the gaseous experiment and partly to the matrix effect on the trapped NO_2 molecules. We have as yet no reasonable explanation for the presence of the lines *d*, *e*, and *f*.

NO

No spin resonance was observed for the NO molecule trapped in an argon matrix at liquid helium temperature. This result is certainly not surprising, since NO would be almost entirely in the nonparamagnetic $^2\Pi_{1/2}$ state at this temperature. Accordingly, another experiment was done in which NO was deposited in a CO_2 matrix at liquid nitrogen temperature, at which temperature the $^2\Pi_{3/2}$ state was expected to have an appreciable population. Nevertheless, the result of the observation was also negative. We believe that the failure to observe resonance results from crystalline anisotropy of the matrix field, which in the case of a Π -state molecule may be sufficient to smear out the resonance lines.

O_2

Spin resonance lines were not observed for oxygen trapped in argon at liquid helium temperature. Two possible explanations for the absence of resonance lines were suggested: (1) Since O_2 in the free state can occupy only odd rotational states, freezing the molecule in a solid could result in a hindered rotation, in which case the fluctuating coupling between molecular rotation and electron spin might broaden the resonance below detection; (2) The crystalline field of the matrix could split the $^3\Sigma$ levels of O_2 to produce a singlet ground level in which case resonance absorption could not be observed with our apparatus.

Recent studies on oxygen trapped in a β -quinol clathrate have clarified the situation regarding O_2 resonance observations in favor of the second possibility mentioned above. Meyer, O'Brien, and Van Vleck¹⁹ measured the magnetic susceptibility of O_2 down to 0.25°K and explained their results by assuming that rotation of the molecule was hindered by a potential barrier. To fit the experimental data they required an effective coupling constant of 4.15°K to describe the spin-molecule axis interaction energy. This corresponds to a zero-field splitting of the $^3\Sigma$ levels of 86.5 kMc/sec. More recently, electron spin resonances for O_2 at 4.2°K in a β -quinol clathrate single crystal have been observed by Foner and Meyer.²⁰ The resonance lines observed at 37 kMc/sec and 71 kMc/sec with pulsed magnetic fields indicate a large zero-field splitting of the oxygen energy levels confirming the magnetic susceptibility results. Our negative result with O_2 is, therefore, rather

¹⁹ Meyer, O'Brien, and Van Vleck, Proc. Roy. Soc. (London) A243, 414 (1958).

²⁰ Simon Foner, Lincoln Laboratory, Massachusetts Institute of Technology (private communication).

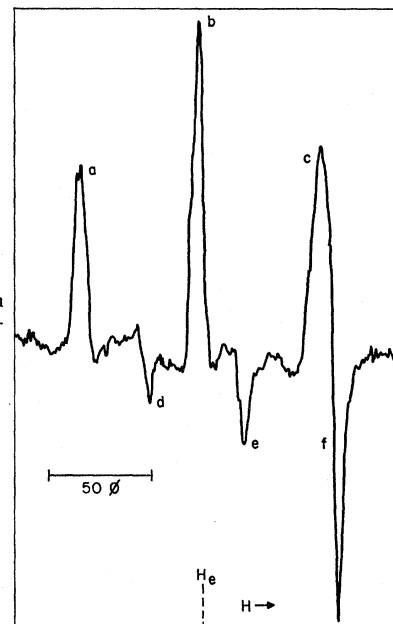


FIG. 12. Spectrum of NO_2 in argon matrix.

easily explained. With our relatively low microwave frequency (9 kMc/sec), rather high magnetic fields would be required to attain resonance. Even under these conditions, the random orientation of the crystals in our samples probably would smear out the resonance lines so that they would not be observable.

V. MATRIX FIELD EFFECTS ON SPIN RESONANCE PROPERTIES OF TRAPPED RADICALS

When a free radical is trapped in a solid matrix, there is an interaction between the radical and its environment. This interaction, in spin resonance experiments, manifests itself in deviations of the spectrum of a trapped radical from that of a free radical. We are interested in comparing the effects of different matrices on the spin resonance properties of a radical and, wherever possible, evaluating these effects on the basis of the known properties of the radical in its free state.

In discussing matrix effects, it would be desirable to be able to specify in detail the solid-state structure in the neighborhood of the radicals. Unfortunately, such a description is not available. It is not known with certainty whether the samples, prepared by condensation of molecular beams on the liquid helium cooled sapphire rod, are amorphous, crystalline or a combination of both. The samples probably consist of many randomly oriented microcrystals possibly joined by amorphous material. The crystals may have different structures corresponding to various solid modifications which can exist at these temperatures. The measured effect of a matrix on a radical may, therefore, be considered as the result of averaging the crystalline effects over all possible orientations.

In order to study matrix field effects in a systematic way, we have taken H, N, and CH_3 as representative

TABLE IV. g_J factors and hyperfine coupling constants (A) of H, N, and CH_3 in various matrices.^a

Free radical species	Matrix	g_J	A (Mc/sec)	Deviation of A from free value
H	free	2.002256(24)	1420.40573(5)	
	H ₂	2.00230(8)	1417.11(20)	-0.23%
	A	2.00220(8)	1413.82(40)	-0.46%
	CH ₄	2.00207(8)	1411.09(32)	-0.66%
N	free	2.00215(3)	10.45(2)	
	H ₂	2.00202(8)	11.45(8)	9.6%
	N ₂	2.00200(8)	12.08(12)	15.6%
	CH ₄	2.00203(8)	13.54(22)	29.5%
CH ₃	free	
	H ₂	2.00266(8)	65.07(13)	...
	A	2.00203(8)	64.64(20)	...
	CH ₄	2.00242(8)	64.39(18)	...

^a The numbers in parentheses indicate experimental and/or conversion errors in the last figures of the associated values.

(zero orbital momentum) free radicals and put each one individually into a series of representative matrices, namely H₂, A or N₂, and CH₄. These matrices have rather different binding energies (Van der Waals' energies). The matrix effects on the resonances of the radicals are conveniently discussed by considering the spectral parameters g_J , A , and line width.

A. g_J and A

The quantities g_J and A are calculated by using the experimental data on the resonance fields of spectral lines at a constant microwave frequency. The results of these calculations are given in Table IV.

We note that the variation of the g values with matrices is rather small for all three radicals, with a slight tendency of decreasing g_J with increasing binding energy. This implies that the spin-orbit coupling induced by the matrix field is exceedingly small. The variation of the hyperfine coupling constant A is interestingly different for the three radicals. In the cases of H and N, the deviation of A for a trapped atom from that for a free atom increases with the binding energy but in opposite directions for the two atoms. Furthermore, the percentage deviation of the coupling constant for H is very much smaller than for N. This situation may be interpreted qualitatively in the following way. A free hydrogen atom has a pure $1s$ wave function having maximum density $|\psi(0)|^2$ at the nucleus. Any matrix perturbation resulting in the admixing of other orbitals would tend to lower the density function at the nucleus. On the other hand, a free nitrogen atom is in a $^4S_{3/2}$ state with three p -electrons having zero density at the nucleus as a first-order approximation and having a small density when one considers configuration interaction. It seems to us, that under these conditions a matrix perturbation has a larger probability of increasing the density function at the nucleus than of decreasing it. Also, when the

coupling constant is initially small for a free atom, small changes in electron density at the nucleus can easily cause large percentage changes in A .

In the case of CH_3 , while there are no free-state data for comparison, the variation of A among the matrices is exceedingly small. In this connection, we have been puzzled by recent reports of CH_3 spectra in which the line spacing was substantially different from ours. An over-all spread for the CH_3 quartet of 80 oersteds has been reported²¹ for CH_3 produced by ultraviolet irradiation of an 0.1M solution of toluene in EPA (ether, isopentane, and alcohol) at liquid nitrogen temperature. We deposited CH_3 radicals in EPA at liquid helium temperature and obtained a quartet spread of 69.9 oersteds, which is very close to the quartet spread found in the other matrices. It is difficult to explain the 15% discrepancy between the results. Since the experiments were run at different temperatures, some of the difference might be attributed to a temperature effect, although we did not observe such an effect in a limited warmup experiment. It appears from our data that the spacing of the CH_3 lines is rather insensitive to environment and can be used to identify this radical in a variety of matrices.

B. Line Width

The theory for the width and shape of spin resonance lines of trapped free radicals is too involved to permit an exact treatment. It is complicated by spin-lattice relaxation, spin density, matrix anisotropy, intensity saturation, rate of passage, and the modulation parameters used in observation. The observed shapes of spectra lines are generally neither Gaussian nor Lorentzian. They are, however, close enough to Gaussian that we shall assume that they are so for our discussions. The line width parameter used here is the usual $\Delta H_{1/2}$ (width at half-intensity points).²² Table V lists the values of $\Delta H_{1/2}$ for H, N, and CH_3 in various matrices. These line widths should be regarded as typical values. Experimentally, the half-width is not a well-controlled parameter and there is appreciable variation among the values obtained in various experiments.

We note in Table V that for a given radical there is a marked broadening of the line as the matrix binding energy increases in going from H₂, through A or N₂, to CH₄. Furthermore, the line widths for the three radicals are rather comparable when they are trapped in the same matrix. It appears that the line widths for the free radicals are more conditioned by the nature of the matrices than by the properties of the radicals. We shall discuss qualitatively the pertinent factors which play a part in determining line shape and width.

²¹ H. N. Rexroad and W. Gordy, Bull. Am. Phys. Soc. Ser. II, 2, 227 (1957).

²² For all spectral lines that appear as derivative curves, the measured width between the maximum and minimum slopes (ΔH_{MS}) is converted into $\Delta H_{1/2}$ by the relation $\Delta H_{1/2}/\Delta H_{MS} = 1.178$ for a Gaussian shape.

Dipolar Broadening

Dipolar broadening is caused by electron spin interactions between neighboring radicals. Using a result of Kittel and Abrahams,²³ the half-width due to dipolar broadening can be expressed by

$$\Delta H_{\frac{1}{2}} \simeq 2 \times 10^{-19} n \text{ oersteds}, \quad (14)$$

where n = number of spins per cc (spin density). Dipolar broadening effects were studied in the case of hydrogen atoms in H_2 . If it is assumed that the line width is solely due to dipolar effect, then it should increase directly with spin density. Even though the spin density is not known in our experiment, the ratio of spin densities in two independent depositions can be determined from the ratio of the integrated absorption intensities, provided the sample volumes are the same. In a particular experiment, the width of the hydrogen line increased by a factor of 1.5 for a spin density increase of roughly a factor of 10. This evidence supports the previously expressed view that the line width is largely controlled by the matrix. The highest spin density in that experiment can be determined from the increase in the line width. The estimated dipolar broadening, 0.7 oersted, leads to a spin density of approximately 4×10^{18} /cc. As the density of solid hydrogen is known, we get a figure of 0.01% for the concentration of hydrogen atoms in its molecular matrix. This figure does not represent the highest concentration achievable for hydrogen atoms, as we have made no serious attempt to obtain highly concentrated samples.

Spin-Lattice Relaxation

Let T_1 denote the spin-lattice relaxation time and T_2 the spin-spin relaxation time in Bloch's notation.²⁴ If $T_1 \gg T_2$, as often happens with paramagnetic species at very low temperatures, the line shape or width is usually conditioned by T_2 in the absence of intensity saturation. However, the longer T_1 is, the easier it becomes for the line to be saturated at a given microwave field.

Confining our attention to the case of hydrogen atoms, a hydrogen line shows a marked saturation effect at a microwave field $H_1 = 5 \times 10^{-3}$ oersted. This implies that the saturation parameter $S = (\gamma H_1)^2 T_1 T_2$ is roughly unity. From our data on dipolar broadening we can calculate T_2 from the relationship $\Delta H_{\frac{1}{2}}$ (dipolar) $= 2/\gamma T_2 = 2\hbar/g\mu_0 T_2$, and find $T_2 \sim 10^{-7}$ sec. This leads to a value of T_1 of the order of 10^{-3} sec. Such a value of T_1 is also derived from other experimental evidence. When field modulation at an angular frequency ω_m is used, the conditions $\omega_m T_1 \ll 1$ and $\omega_m T_1 \gg 1$ are usually taken to define the so-called slow-passage and fast-passage regions. In the present experiment a modulation frequency of 400 cps is used, so that with an assumed

TABLE V. $\Delta H_{\frac{1}{2}}$ (oersteds) for H, N, and CH_3 in various matrices.

Radical	H_2 matrix	A or N_2 matrix	CH_4 matrix
H	1.4	2.5(A)	4.7
N	1.6	2.3(N_2)	5.6 ^a
CH_3	1.4	3.7(A)	4.5

^a Estimated from partially resolved lines.

$T_1 = 10^{-3}$ sec we have $\omega_m T_1 = 2.5$ which fits into an intermediate-passage region. The departure of the hydrogen line presentation from the usual absorption-derivative curve, as has been noted before, can be interpreted as an intermediate-passage phenomenon. Furthermore, when the quadrature component of the absorption signal at the modulation frequency becomes comparable to the in-phase component, as has been observed with hydrogen lines, we can follow Redfield's method²⁵ to determine T_1 by noting that $\omega_m T_1 = I(90^\circ)/I(0^\circ)$, where I denotes the intensity at resonance. The result of one such determination gave the value 0.5×10^{-3} sec for T_1 , which is in essential agreement with our preceding discussions.

The intensity distribution of the lines in a spin resonance spectrum may change markedly with microwave power. This is a saturation phenomenon that can arise when there are differences in the relaxation times associated with the energy levels involved in the transitions. Such a phenomenon is clearly involved, for example, in the deuterium atom experiments. As a possible mechanism for spin-lattice relaxation in the case of hydrogen and deuterium atoms, Abragam²⁶ proposed a model based upon hyperfine coupling in the following manner. In the hyperfine interaction term $A \mathbf{J} \cdot \mathbf{I} = A[J_z I_z] + \frac{1}{2} A[J_+ I_- + J_- I_+]$, the operator in the second term on the right-hand side has matrix elements connecting any two levels having the same M_F , i.e., $M_J + M_I$. A radiationless transition between any two such levels acts as an agent for the restoration of thermal equilibrium. They are, therefore, spin-lattice relaxation paths for the energy levels considered. Figures 13 and 14 show, respectively, diagrams for the hyperfine energy states of hydrogen and deuterium atoms in a magnetic field with the radiation and relaxation paths indicated. Assuming that all relaxation paths have equal effectiveness, then for a given radiative resonance transition, a relaxation path taking spins from the upper energy level is equivalent to a path delivering spins to the lower energy level. We note that the two hydrogen lines illustrated in Fig. 13 are equally relaxed, whereas the center line in the deuterium triplet in Fig. 14 is relaxed twice as fast as either of the side lines. This means that the hydrogen lines should be equal in in-

²⁵ A. G. Redfield, Phys. Rev. **98**, 1787 (1955). There is some question whether the theory is strictly applicable to the present case. We, therefore, consider the result by Redfield's method as confirmatory evidence for the order-of-magnitude calculation of T_1 rather than a more accurate determination of T_1 .

²⁶ A. Abragam (private communication).

²³ C. Kittel and E. Abrahams, Phys. Rev. **90**, 238 (1953).

²⁴ F. Bloch, Phys. Rev. **70**, 460 (1946).

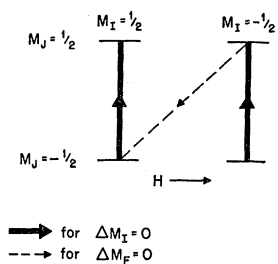


FIG. 13. Spin-lattice relaxation by hyperfine coupling for hydrogen atoms.

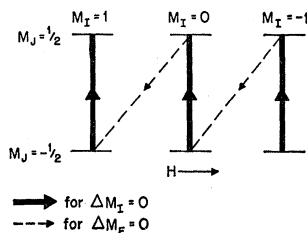


FIG. 14. Spin-lattice relaxation by hyperfine coupling for deuterium atoms.

tensity with or without saturation, but the deuterium spectrum should have a stronger (also somewhat narrower) center line, except when saturation is negligible.

Abraham's theory on the saturation effect has, to a large extent, been verified by the experimental results for the deuterium atom. We observed that the ratio of the intensity of the center line to that of either side line continuously decreased from about 4 to 1.5 as the microwave power was reduced. The fact that the center line in deuterium remained sensibly stronger than either side line even at very low power level indicates that the theory does not fully explain the observations and that other mechanisms may be involved.

Anisotropic Broadening

The line widths can be considered as the result of three effects: (1) dipolar interaction; (2) spin-lattice relaxation; and (3) crystalline anisotropy. We have shown that for the spin densities encountered in this paper, dipolar broadening produces only a small effect. Since the spin-lattice relaxation time is large compared to the spin-spin (dipolar) relaxation time, it is also a small contributor to the line width. It, therefore, seems most probable that the observed line widths are largely the result of anisotropic broadening by the matrix field. The line widths for the radicals H, N, and CH_3 were comparable when trapped in the same matrix, indicating that the line width was more affected by the nature of the trapping matrix than by the characteristic properties of the individual radicals. The observed lines in our polycrystalline matrices are the result of averaging resonances over all crystallographic orientations. The

anisotropy due to the crystalline field, contained in the orientation dependences of g_J and A in a single crystal, is reflected in our experiments as a broadening of the resonance lines.

CONCLUSION

A systematic study has been made of the electron spin resonance spectra of atomic and molecular free radicals under well-defined experimental conditions. The effects of the matrix field on g_J , hyperfine coupling constant, line width and line shape have been investigated by depositing the radicals in matrices with different binding energies.

Cases where the electron spin resonance method, as currently applied, has failed to detect radicals have also been considered. It appears that radicals with orbital angular momentum may escape observation because of matrix field anisotropy and that radicals with an even number of electrons may not be observed because of crystalline field splitting resulting in a singlet ground level. The use of a single crystal for the matrix is a means of alleviating the difficulty of anisotropic broadening. There exists a need for developing techniques for the preparation of single crystals containing selected unstable free radicals.

In addition to the identification and study of the properties of trapped free radicals, the electron spin resonance method could be extended to non-stationary chemical systems. The investigation of free radicals in excited states may prove to be rewarding. The diffusion of radicals at low temperatures could be followed in a quantitative way by observing the decrease in resonance signal resulting from radical recombination. The chemical kinetics of radical reactions in the solid state is also an interesting area for exploration with this method.